Ph.D. Dissertation

Identification of diagnostic biomarkers for pediatric Moyamoya disease based on plasma-derived extracellular vesicle microRNA

혈장 유래 세포밖소포체 마이크로RNA 기반
소아 모야모야병의 진단 바이오마커 발굴

August 2022

Graduate School of Medicine
Seoul National University
Translational Medicine Major

Eun Jung Koh

Identification of diagnostic biomarkers for pediatric Moyamoya disease based on plasma-derived extracellular vesicle microRNA

Advisor: Seung-Ki Kim

Submitting a Ph.D. Dissertation of
Eun Jung Koh
April 2022

Graduate School of Medicine
Seoul National University
Translational Medicine Major

Eun Jung Koh

Confirming the Ph.D. Dissertation written by
Eun Jung Koh
July 2022

Chair	Hee-Soo Kim	(Seal)
Vice Chair	Seung-Ki Kim	(Seal)
Examiner	Jong Hee Chae	(Seal)
Examiner	Won-Sang Cho	(Seal)
Examiner	Jung Won Choi	(Seal)

혈장 유래 세포밖소포체 마이크로RNA 기반 소아 모야모야병의 진단 바이오마커 발굴

지도 교수 김 승 기

이 논문을 의학박사 학위논문으로 제출함
2022년   4월

서울대학교 대학원
의학과 중개의학전공
고 은 정

고은정의 의학박사 학위논문을 인준함
2022년   7월

위 원 장	김 희 수	(인)
부위원장	김 승 기	(인)
위 원	채 종 희	(인)
위 원	조 원 상	(인)
위 원	최 정 원	(인)

Abstract

Background. Moyamoya disease (MMD) is a chronic occlusive cerebrovascular disease known to be a major cause of stroke in children. Emerging evidence suggests that circulating extracellular vesicles (EVs) containing miRNAs in cerebrovascular disease plays a significant role in intercellular communication by delivering RNA cargo involved in biological processes. This study aimed to investigate the specific miRNAs loaded into MMD plasma-derived EVs, followed by identification of their roles and mechanisms.

Methods. Plasma-derived EVs were isolated from normal control and MMD patients. EVs were characterized using transmission electron microscopy, nanoparticle tracking analysis, ExoView and western blot. Profiling of miRNAs in EVs were determined using NanoString nCounter miRNAs analysis system and validated using ExoView and RT-qPCR. Endothelial colony forming cells (ECFCs) from MMD were isolated and the miRNA inhibitor was transfected to assess the cell viability, guanosine triphosphatase (GTPase) activity, and tubule formation.

Results. There was no significant difference in size and distribution of EVs between normal and MMD EVs. However, the total number was higher, with CD81 and CD9 were lower and CD63 was higher in MMD EVs. miRNA profiling demonstrated that miR-512-3p were significantly upregulated in MMD EVs. Target prediction analysis of miR-512-3p showed that Rho guanine nucleotide exchange factor 3 (ARHGEF3) was downregulated by miR-512-3p in MMD ECFCs. Inhibition of miR-512-3p in ECFCs reduced miR-512-3p in EVs as well as ECFCs, and increased ARHGEF3 expression. The increase in ARHGEF3 through the inhibition of upregulated miR-512-3p in MMD EVs, which can restore dysfunction of tubule formation by activating GTPase.

Conclusion. Our study implies that MMD EV miR-512-3p is correlated with the metabolism of ECFCs and may affect defective angiogenesis.

Student Number: 2017-35670

Contents

List of Figures and Tables

List of Abbreviations

Analysis of variance (ANOVA)

Area under the ROC curve (AUC)

Cerebrospinal fluid (CSF)

Differentially expressed messenger RNAs (DEmRNAs)

Differentially expressed microRNAs (DEmiRNAs)

Endothelial cell (EC)

Endothelial colony-forming cells (ECFCs)

Enzyme-linked immunosorbent assay (ELISA)

Ethylenediaminetetraacetic acid (EDTA)

Extracellular vesicles (EVs)

Fold change (FC)

Glucoside Xylosyltransferase 1 (GXYLT1)

Guanosine diphosphate (GDP)

Guanosine triphosphate (GTP)

Guanosine triphosphatase (GTPase)

Induced pluripotent stem cell derived endothelial cell (iPSEC)

Insulin like growth factor 1 (IGF-1)

Internal carotid artery (ICA)

Kyoto encyclopedia of genes and genomes (KEGG)

Magnetic resonance imaging/angiography (MRI/A)

Mammalian target of rapamycin (mTOR)

Matrix-metalloproteases (MMPs)

Messenger RNA (mRNA)

MicroRNA (miRNA)

Mitogen-activated protein kinase (MAPK)

Moyamoya disease (MMD)

mTOR complex 2 (mTORC2)

Nanoparticle tracking analysis (NTA)

Negative control (NC)

Optical density (OD)

Phosphatase and tensin homolog (PTEN)

Phosphoinositide 3-kinase (PI3K)

Real-time quantitative polymerase chain reaction (RT-qPCR)

Receiver operating characteristic (ROC)

Rho Guanine Nucleotide Exchange Factor 3 (ARHGEF3)

Signal transducer and activator of transcription 3 (STAT3)

Speckle-type BTB/POZ protein (SPOP)

Survival of motor neuron-related-splicing factor 30 (SMNDC1)

The serine/threonine Rho-associated kinases (ROCKs)

Thymocyte selection-associated high mobility group box (TOX)

Transforming growth factor (TGF)

Transmission electron microscopy (TEM)

Vascular endothelial growth factor (VEGF)

Introduction

Moyamoya disease (MMD) is a progressive cerebrovascular disorder characterized by bilateral occlusion of the supraclinoid internal carotid artery (ICA) and its major branches. Subsequently, fine collateral networks develops, particularly adjacent to the occlusion site in the deep areas of the brain (1). Transient ischemic attack and ischemic stroke are the main presenting symptoms in childhood. Both symptoms are related to the stenosis and occlusion of the ICAs. In adulthood, rupture of fragile collateral vessels causes hemorrhagic stroke (2).

Stroke-related neurological sequelae have a long-term negative impact on a patient's quality of life. Early identification and treatment of MMD are critical. Currently, MMD is diagnosed with conventional cerebral angiography as a confirmatory test. Sedation is essential in pediatric patients because the procedure is invasive. Although magnetic resonance imaging/angiography (MRI/A) is a non-invasive screening test, it can take time to complete. Furthermore, because of its limited specificity, it is difficult to distinguish MMD from other cerebrovascular disorders (2). MMD develops slowly. Therefore, it may not be detected with a single MRI/A. In addition, it is expensive to perform MRI/A as a screening test for asymptomatic people who have MMD patients in their families.

There is a growing desire for easy, practical, and safe diagnostic tests. Recently, the concept of liquid biopsy has emerged in diseases such as cancer. Liquid biopsy aims to diagnose a disease at an early stage before direct surgical biopsy by detecting disease-specific genome, transcriptome, and proteome in the patient's body fluid. This concept can also be applied to the field of cerebrovascular disease. Retrieving tissue of affected cerebral arteries during surgery is difficult in MMD. Acquiring indirect information from body fluids such as blood, cerebrospinal fluid, and urine can be helpful in diagnosis. Plasma is the most commonly accessible body fluid. Given the association of MMD with blood vessels, characterizing the

molecular alterations in plasma from patients may provide insight into the disease (3).

MicroRNAs (miRNAs) are regulatory small non-coding RNAs of approximately 22 nucleotides produced by all cells in the body. The classic function of miRNAs is inhibiting target messenger RNA (mRNA) translation or increasing mRNA degradation. Some miRNAs have the opposite effect, activating transcription and upregulating protein expression, by acting through non-canonical pathways. Similar to mRNAs, the miRNA expression profile serves as a signature of cell identity (4).

miRNAs are exported and imported by cells through mechanisms involving vesicle trafficking and protein carriers. Extracellular vesicles (EVs) secreted from certain cell are taken up by other cells, followed by the release of their cargo into target cells (5). EVs are isolated from different sources such as blood, urine, breast milk, and saliva. EVs contain different types of molecules including DNA, RNA, miRNA, lipids, and proteins. The membrane of EV protects its contents against degradation by nucleases, proteases, fluctuations in pH and osmolarity. The intraluminal content is relatively stable, therefore EVs may provide a more consistent source of biomarker than whole unfractionated body fluid (6). The contents of EV are transmitted through intercellular or inter-tissue communication. EV miRNAs are considered as potential diagnostic biomarkers because of their easy access and stability (7).

In this study, we investigated miRNA profiling of plasma-derived EVs of pediatric MMD patients. We also sought to determine the role of genes regulated by miRNAs in the pathophysiology of MMD.

Materials and Methods

Human blood and cerebrospinal fluid (CSF) collection and preparation

Peripheral blood was obtained from MMD patients (N=19) and healthy volunteers (normal, N=13) with informed consent under Seoul National University Hospital Institutional Review Board (IRB No. 1904-096-1027) approved (Table 1). All MMD patients confirmed diagnoses based on cerebral angiography. Blood of patients was collected from the radial arterial catheter under general anesthesia for indirect bypass surgery. Since it is ethically impossible to recruit the blood of healthy children, blood from young adults with no history of stroke, high blood pressure, chronic disease and smoking was recruited as normal group. The blood was acquired through collection of whole blood in ethylenediaminetetraacetic acid (EDTA) tubes. 10 ml of plasma was extracted from the total 40 ml of blood and the remaining 30 ml was used to isolate mononuclear cells. After blood collection, the samples were spun at 2,500 rpm for 15 min. Plasma isolated from blood was then transferred into a 15 ml conical tube and spun at 2,000 g for 20 min. 1.2 ml of plasma was recovered from each sample and stored in a sterile cryogenic vial at -20°C. CSF samples were collected from cortical subarachnoid space during indirect bypass surgery in MMD patients (N=15). We set children with hydrocephalus as a control group (N=8) of CSF experiments. Brain tumor, infection, and other potential secondary causes of hydrocephalus were ruled out. CSF samples of control group were collected from ventricular catheter during shunt operation or extracranial ventricular drainage. CSF was centrifuged at 1,000 g for 20 min, then 10,000 g for 30 min at 4°C to remove cells and debris. CSF was immediately frozen at -80°C until use.

Table 1. Clinical characteristics and experimental usage of blood from Moyamoya disease (MMD) patients and normal group

	Sex	Age (yr)	Symptoms	MRI finding	Suzuki grade (R/L)	RNF213 p.R4810K genotype	TEM	NTA	ExoView	EV miR-512-3p expression
MMD1	M	9	TIA	No infarct	2/2	G/A			○	1.928819215
MMD2	F	6	TIA	No infarct	2/2	G/A			○	3.156084519
MMD3	F	11	TIA	No infarct	1/2	G/A			○	3.021535146
MMD4	F	10	TIA	No infarct	3/3	G/G			○	2.580167651
MMD5	M	11	TIA	No infarct	4/4	G/A				3.693157131
MMD6	F	11	Involuntary movement	No infarct	3/4	G/A			○	3.138955658
MMD7	F	5	Hemiparesis	Infarct	4/4	G/A				2.658588127
MMD8	F	3	Hemiparesis	Infarct	3/3	G/G				2.623743366
MMD9	F	7	TIA	No infarct	3/2	G/A			○	3.86173166
MMD10	F	1	seizure	Infarct	NA	G/G				4.222672333
MMD11	F	7	TIA	No infarct	4/4	G/A			○	4.486165913
MMD12	M	5	TIA	No infarct	3/2	G/A		○	○	0.753754039
MMD13	M	9	TIA	No infarct	4/4	G/A	○		○	1.253827642
MMD14	M	9	Hemiparesis	Infarct	3/3	G/A	○			3.226297432
MMD15	M	5	TIA	No infarct	2/4	A/A				
MMD16	F	4	TIA	No infarct	3/3	G/A				
MMD17	M	2	Hemiparesis	Infarct	4/4	A/A	○	○	○	
MMD18	M	8	TIA	No infarct	4/4	G/A	○	○	○	
MMD19	M	6	TIA	No infarct	4.4	G/A				
N1	M	21				G/G			○	2.642688
N2	F	21				G/G				-1.749982519
N3	M	21				G/G			○	2.382594519
N4	M	22				G/G				1.161997092
N5	M	21				G/G			○	2.153851518
N6	F	24				G/G	○	○		2.78717704
N7	F	24				G/G		○		1.291281646
N8	M	19				G/G		○		2.471821599
N9	M	25				G/G				2.287411667
N10	F	25				G/G	○			2.809203346
N11	F	23				G/G				
N12	M	25				G/G			○	
N13	M	25				G/G			○	

Abbreviations: MMD, Moyamoya disease; R, Right hemisphere; L, Left hemisphere; RNF213, Ring Finger Protein 213 gene; TEM, Transmission electron microscopy; NTA, Nanoparticle tracking analysis; EV, Extracellular vesicle; TIA, Transient ischemic attack; NA, Not available.

Cultures of endothelial colony-forming cells (ECFCs)

ECFCs were isolated from the peripheral blood of as described previously (8, 9). ECFCs were cultured in endothelial cell growth medium (EGM-2, Clonetics, San Diego, CA, USA) and maintained at 37°C in a humidified atmosphere containing 5% CO_2 and used under passage 6 for further experiment. ECFCs were characterized by flow cytometry and fluorescence analysis before use in further experiment.

Isolation of EVs in plasma, CSF, and conditioned media of ECFCs

EVs in plasma from MMD patients and normal group were isolated using total exosome isolation kit (Invitrogen, Carlsbad, CA, USA) according to manufacturer's protocol. Briefly, frozen plasma samples were equilibrated to room temperature. After centrifugation of 1.2 ml plasma at 10,000 g for 20 min, residual cells and cell debris were removed. Supernatant (1 ml) was transferred into a new tube and 0.5 volumes of 1×PBS was added. For remove the bulk of protein from plasma, added 0.05 volumes of protease K and incubated at 37°C for 10 min. Then, 0.2 volumes of exosome precipitation reagent added into the tube. The tube was thoroughly mixed and incubated at 4°C for 30 min. This was followed by centrifugation at 10,000 g for 5 min, after which the supernatant was discarded and EVs were contained in a pellet.

EVs from CSF were isolated using Exo2D™ (Exosome Plus, Suwon, Korea) according to the manufacturer's instructions. 4 ml of CSF were mixed with 0.8 ml of extraction reagent, incubated for 1 hr at 4°C and centrifuged at 3,000 g for 30 min at 4°C.

EVs in conditioned media of ECFCs were isolated by miRCURY exosomes isolation kit (Exiqon, MA, USA) as described previously (10). Briefly, ECFCs were maintained for 3 days until 90% confluency in EGM-2 with exosome free FBS (System Biosciences, CA, USA). 10 ml of conditioned media was harvested

and centrifuged at 3200 g for 15 min to remove residual cells and cell debris. Supernatant (8 ml) was transferred into a new tube and precipitation buffer was added as 5:2. The tube was incubated at 4°C for 1 hr and spun at 3,200 g for 30 min.

Transmission electron microscopy (TEM)

The morphology and size of EVs in plasma from MMD patients (N=4) and normal group (N=2) was identified using TEM (Table 1). Briefly, EVs were mixed with 4% paraformaldehyde and embedded in a formvar-carbon-coated grid at room temperature. Then, the EVs were washed, fixed, stained, embedded, dried and visualized with TEM (JEOL, Peabody, MA, USA).

Nanoparticle tracking analysis (NTA)

To measure the size, distribution, and concentration of plasma-derived EVs, NTA with a NanoSight NS3000 (Malvern Instruments, Malvern, UK) was conducted (11). EVs in plasma from 3 MMD patients and 3 normals were used (Table 1). Briefly, EVs were diluted with autoclaved distilled water to obtain optimum particle concentration of 20-150 per one frame and EVs were diluted with 1 ml. The samples were added into a chamber held on a light microscope and the images were captured in triplicate over a 60 sec period at 10 frames/sec. The record provided the distribution of the number of particles per unit volume by size.

ExoView analysis

The physical and biological properties of EVs was analysed using ExoView system (NanoView Biosciences, Brighton, MA, USA) according to the manufacturer's protocol. EVs in plasma from 11 MMD patients and 5 normals were used (Table 1). For detection of tetraspanins as EV markers in plasma-derived EVs, diluted plasma (1:10) or conditioned media (1:5) were incubated overnight on microarray chips (NanoView) coated with capture antibodies for CD81 (Green, NanoView), CD63

(Red, NanoView), CD9 (Blue, NanoView), or negative control IgG1 (NanoView).

For detection of miRNAs in EVs, diluted plasma (1:5) or conditioned media (1:2) were incubated overnight on microarray chips (NanoView) coated with capture molecular beacon for miR-512 (Bioneers, Daejeon, Korea), or negative control (Bioneers). The number of positive particles were quantified using ExoView R100 reader by nScan 2.8.4 acquisition software (NanoView) and the data were analysed using NanoViewer 2.8.11.

Western blotting

Proteins from EVs or ECFCs were extracted with RIPA buffer. Primary antibodies were employed as follows: Flotillin-1 (1:1000, Abcam, Cambridge, MA, USA), CD63 (1:1000, Abcam), Cytochrome C (1:1000, Cell Signaling Technology, Danvers, MA, USA), CD9 (1:1000, Abcam), Calnexin (1:1000, Cell Signaling Technology) and β-actin (1:10,000, Sigma-Aldrich, St. Louis, MO, USA). Flottilin1, CD63, and CD9 were used as positive EV markers. β-actin, cytochrome C, and calnexin were used as negative control markers for EV. The membranes were incubated with a secondary antibody conjugated with horseradish peroxidase and visualized using the enhanced Novex™ ECL Chemiluminescent Substrate Reagent Kit (Life Technologies, CA, USA).

RNA isolation

Total RNAs including miRNAs in EVs from plasma of MMD patients and normal group were isolated using a miRNeasy kit (Qiagen, Hilden, Germany). Before analysis, the quality and quantity of all purified RNAs were confirmed using a Nanodrop 2000 Spectrophotometer and an Agilent 2100 Bioanalyzer (Agilent Technologies, Santa Clara, CA, USA).

NanoString miRNA analysis

NanoString nCounter (NanoString Technologies, Seattle, WA, USA) using 800 human v3 miRNA expression assays employed to analyse EV miRNAs. A total of 100 ng of total RNAs per sample from isolated plasma-derived EVs were used as input material, and 3 µl of total volume was used for each sample. Differential expression analysis was performed to identify miRNAs were either upregulated or downregulated. Based on the differentially expressed miRNAs (DEmiRNAs) analysis with fold change (FC) for MMD (N=14) versus controls (N=10), the criteria ($|\log_2 FC| \geq 1$ and $p < 0.05$) for each mappable miRNAs were selected for further analysis.

Integrative analysis of miRNAs and mRNAs

Given the availability of both miRNA NanoString and mRNA array data, integrative analysis was performed. For each miRNA, the target genes were predicted using database TargetScan. The predicted one hundred miRNA-mRNA interactions were connected in a network using program FunRich. To determine whether mRNAs were enriched in biological pathways curated in biological knowledge databases such as Kyoto Encyclopedia of Genes and Genomes (KEGG) and WikiPathways. P values from enrichment analysis were adjusted using the false discovery rate method.

Real-time quantitative polymerase chain reaction (RT-qPCR)

We performed RT-qPCR analysis to validate mRNA and miRNA expression. For the determination of miRNAs expression levels in ECFCs, the miScript SYBR Green qPCR kit (Qiagen) was used with miRNA-specific forward primers (Qiagen). For the validation of mRNAs (ARHGEF3, TOX, PCDH10, PFKP, GXYLT1, MBNL1, ARL5B, SPOP, SMNDC1 and PTBP2), TaqMan® probes were obtained from Applied Biosystems (Applied Biosystems, CA, USA) and performed according to the manufacturer's protocol. The expression levels were normalized

using GAPDH for mRNA and RUN6B for miRNAs.

Transfection of miRNA inhibitor

miRNA inhibitor (antisense inhibitor RNAs) and negative control (NC) miRNA were purchased from Bioneers. MMD ECFCs (N=2) plated in 6-well dish at a density of 2×10^5 cells/well. After 16 hrs, the ECFCs were transfected with miR-512-3p inhibitor (50 nM) or their corresponding NC miRNA using Lipofectamine RNAiMAX (Invitrogen) according to the manufacturer's protocol. The media were replaced to remove transfection reagent after 5 hrs. Transfection efficiency was detected 48 hrs after transfection using RT-qPCR.

Cell viability analysis

Cell viability was assessed using EZ-Cytox cell viability assay kit (Daeil Biotech, Suwon, Korea) according to the manufacturer's protocol. In brief, MMD ECFCs (N=2) were seeded at a density of 1×10^4/well in 96 well plates and incubated for 24, 48 and 72 hrs. The cells were incubated with 10 ul of the Ez-cytox solution for 2 hrs at 37°C. The optical density (OD) was determined at 450 nm using enzyme-linked immunosorbent assay (ELISA) reader. Each experiment was repeated at least three times.

Guanosine triphosphatase (GTPase) activity assay

GTPase activity was measured using a colorimetric GTPase assay kit (Sigma-Aldrich) according to manufacturer's instructions. After transfection of miR-512-3p in MMD ECFCs, the cells were harvested and sonicated in cold assay buffer. Reaction mixtures were contained 20 µl Assay Buffer and 10 µl of 4 mM guanosine triphosphate (GTP), the mixtures incubated with samples for 30 min at room temperature to terminate. The OD was measured at 620 nm using ELISA reader. The GTPase activity (mU/L) was calculated by the following formula: [Pi]

(mM) $\times$ 40 µl $\div$ [10 µl $\times$ reaction time (min)]. This value was corrected by dividing by the protein quantitative value (mg/L). The unit of GTPase activity was expressed as mU/mg in the graph.

Tubule formation analysis

Tube formation was performed using Matrigel (BD Biosciences, NJ, USA). Matrigel was added to 48-well plates and incubated at 37°C. MMD ECFCs (N=2) were seeded at a density of 2 $\times 10^4$/well on Matrigel-coated plates and incubated for 18 hrs at 37°C and 5% CO_2. The developing capillaries were observed and photographed under the inverted phase contrast microscopy (Zeiss, Oberkochen, Germany). Each experiment was repeated at least three times.

Statistical analysis

We used GraphPad Prism version 5 (GraphPad Software, San Diego, CA, USA) to analyse the dataset. Student's unpaired *t*-test was used for comparisons between two groups. One-way or two-way analysis of variance (ANOVA) followed by post hoc Bonferroni test was used for multiple comparisons. A receiver operating characteristic (ROC) curve analysis was performed, and the area under the ROC curve (AUC) was calculated to evaluate the diagnostic value. The optimal cut-off value, sensitivity, and specificity were determined by calculating the Youden index. The heatmap was drawn using MeV 4.9.0. All data are expressed as mean $\pm$ standard deviation (SD). A value of $P < 0.05$ was considered to indicate a significant difference.

Results

Isolation and characterization of plasma-derived EVs from normal group and MMD patients

We compared the characteristics of plasma-derived EVs from normal group and MMD patients. First, TEM showed the typical morphology of EVs, which are round-shaped membrane vesicles with a diameter of 50-200 nm in normal and MMD (Fig. 1A). Second, NTA showed the total number of particles was higher in normal plasma than MMD plasma, but there was no significant difference in size distribution (Fig. 1B). Third, ExoView affinity microarray system exhibited that EV protein markers such as CD81, CD63 and CD9 were observed in both normal and MMD EVs. (Fig. 1C). Notably, we found that there was a difference counting numbers of each marker between normal and MMD EVs. CD81 and CD9 were higher in normal EVs than MMD EVs, while only CD63 was higher in MMD EVs. Western blot analysis revealed that flotillin1 was expressed higher in normal EVs than MMD EVs (Fig. 1D). As expected, β-actin and cytochrome C were not detected at both normal and MMD EVs. CD9 and CD63 were not found, but calnexin and β-actin were detected in both normal and MMD ECFCs (Fig. 1E).
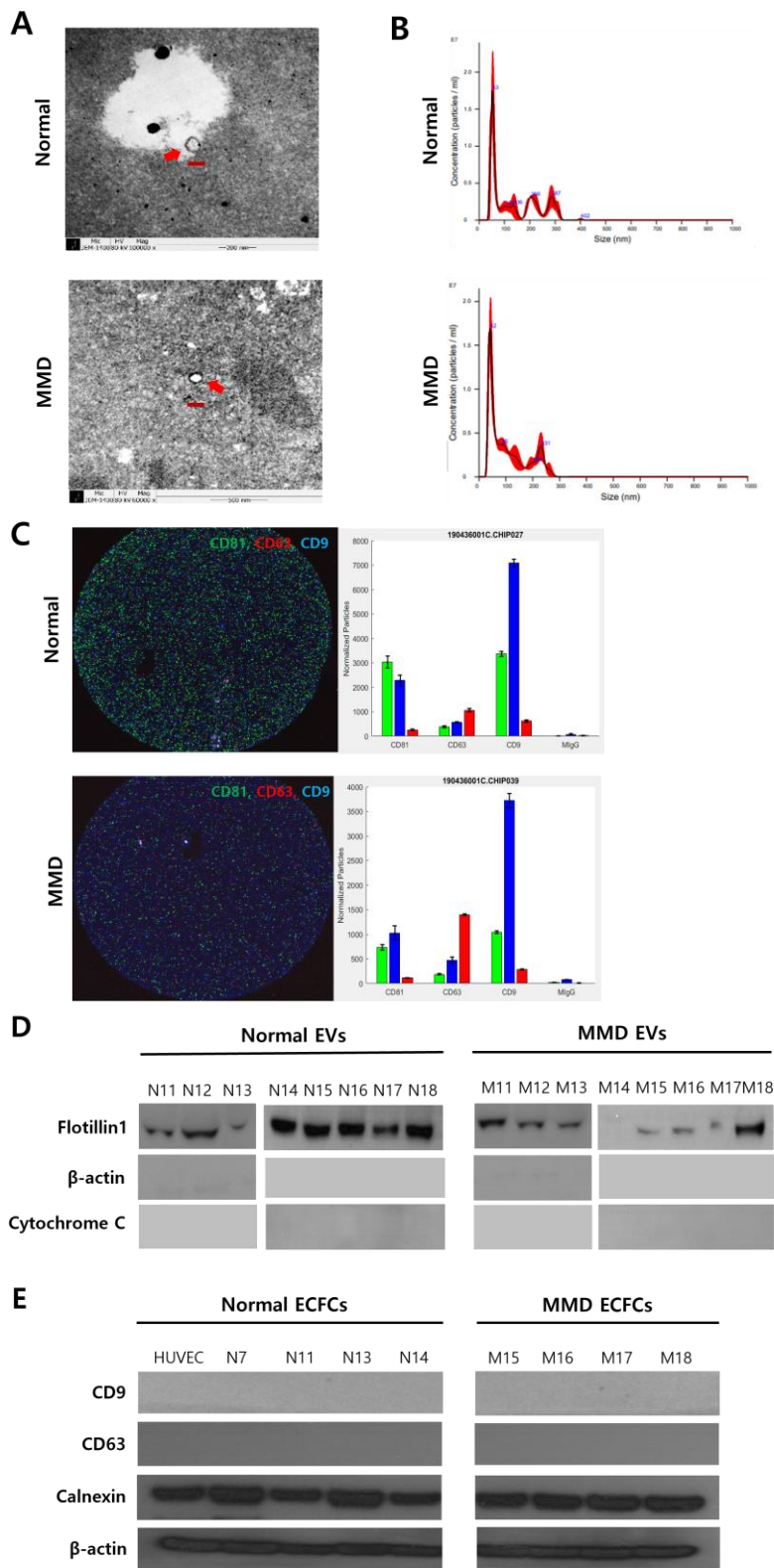
Figure 1. Characterization of plasma-derived extracellular vesicles (EVs) and

endothelial colony-forming cells (ECFCs) from Moyamoya disease (MMD) patients comparing to normal group.

(A) Representative images of transmission electron microscopy. Scale bars, 100nm. (B) Graphs of nanoparticle tracking analysis show particle distribution and the total number of particles. (C) ExoView images reveal enrichment of EV surface markers, CD81, CD63 and CD9. Co-expression of EV markers is assessed by capturing EVs with the indicated secondary fluorescence-labelled antibodies. (D) Immunoblotting shows that flotillin-1 is detected, but ß-actin and cytochrome C are not found in both EVs. Expression of flotillin-1 is higher in normal EVs than in MMD EVs. (E) CD9 and CD63 are not detected, but calnexin and ß-actin are detected in both normal and MMD ECFCs.

Determining of DEmiRNAs in plasma-derived EVs from MMD

NanoString miRNA analysis was employed to identify DEmiRNAs between the normal and MMD EVs. We found that miR-512-3p was the only upregulated miRNA in MMD EVs. On the other hand, miR-320e, miR1268a, miR-3136-5p, miR-3150b-3p, and miR-219a-3p were downregulated (Table 2). We checked the predicted target genes lists of the selected six significant miRNAs and performed a molecular functional analysis on them (Fig. 2A). Unfortunately, the most meaningful content forms the mechanism related to the target genes was unknown. Therefore, we decided to proceed our experiments with an emphasis on miR-512-3p. The robustness of NanoString miRNA analysis data was quantified through ExoView system using a molecular beacon to obtain more elaborate results. EVs were captured by antibodies targeting the CD9 with miR-512-3p molecular beacon, subsequently imaged and quantified. ExoView analysis showed that miR-512-3p was more observed in CD9 captured MMD EVs (Fig. 2B). To evaluate the diagnostic value for miR-512-3p in MMD EVs, we confirmed the ROC curves. miR-512-3p yielded an AUC value of 0.823 in distinguishing MMD patients from normal group (Fig. 2C). Next, miR-512-3p in ECFCs was verified using RT-qPCR. We observed that miR-512-3p was upregulated consistently in MMD ECFCs (Fig. 2D). Further, we wanted to determine whether miR-512-3p expression was likewise elevated in CSF EVs. CSF-derived EVs from control group and MMD patients were captured by antibodies with molecular beacon of miR-512-3p, the most upregulated miRNA, and miR-320e, the most downregulated miRNA (Fig. 2E). The mean value of numbers of miR-512-3p particles in CSF-derived EVs from MMD patients was slightly larger than that from control group, and the mean value of numbers of miR-320e particles in CSF-derived EVs from MMD patients was smaller than that from control group. However, the differences were not statistically significant (both $P>0.05$).

Table 2. Profiling of differentially expressed miRNAs (DEmiRNAs) in plasma-derived EVs from MMD patients.

miRNA	Expression	logFC	AveExpr	t	P.Value
hsa-miR-512-3p	up	1.076588	2.451814	2.138194	0.038527
hsa-miR-219a-2-3p	down	-1.10808	3.092496	-2.28829	0.027362
hsa-miR-3150b-3p	down	-1.1834	1.785484	-2.16975	0.035892
hsa-miR-3136-5p	down	-1.23795	3.519189	-2.48697	0.017058
hsa-miR-1268a	down	-1.3236	3.826419	-2.71337	0.009704
hsa-miR-320e	down	-3.71402	8.325576	-4.43591	6.77E-05

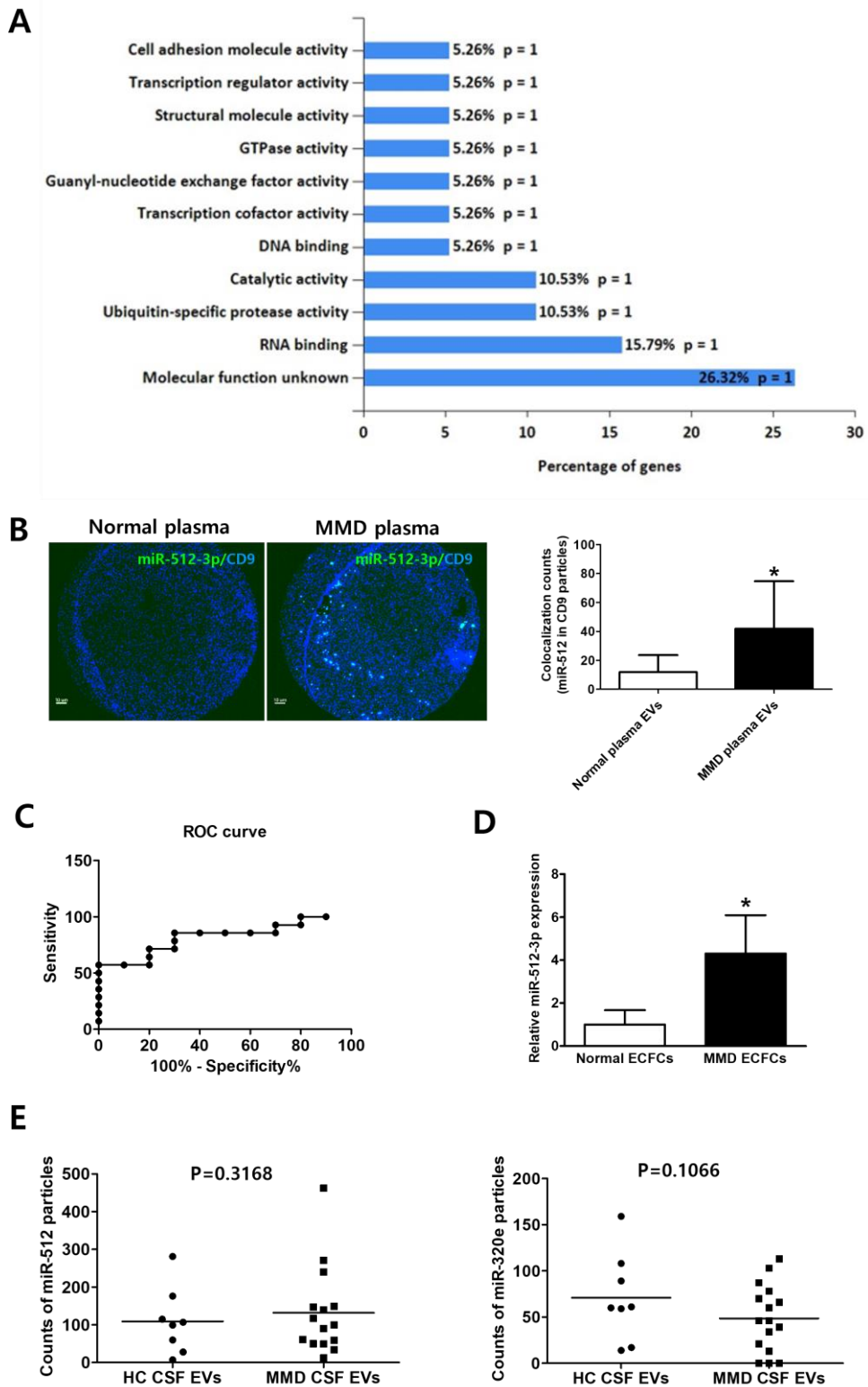Abbreviations: logFC, Log_2 fold change; AveExpr, The average log_2 expression level.

Figure 2. Differential expression of miR-512-3p in EVs from plasma and

cerebrospinal fluid (CSF) of MMD patients.

(A) Molecular functional analysis on target genes of six miRNAs (miR-512-3p, miR-320e, miR1268a, miR-3136-5p, miR-3150b-3p, and miR-219a-3p). (B) ExoView analysis reveal that representative images of plasma-derived EVs providing co-localization information for miR-512-3p (Green) and CD9 (Blue). The normalized number of particles is shown in the bar graphs. Scale bars: 10μm. (C) A receiver operating characteristic (ROC) curve analysis for evaluating the diagnostic power of the miR-512-3p in plasma-derived EVs of MMD patients. miR-512-3p yields the area under the ROC curve (AUC) values of 0.823 with 100% sensitivity and 61.5% specificity. (D) Real-time quantitative polymerase chain reaction (RT-qPCR) shows that the expression level of miR-512-3p in MMD ECFCs compared to normal ECFCs (*: $p < 0.05$). (E) The graphs demonstrate the numbers of captured particles of miR-512-3p and miR-320e by ExoView system in CSF-derived EV from control group (HC: hydrocephalus) and MMD patients.

Identification of the target genes of miR-512-3p in plasma-derived EV from MMD patients

Predicted target genes of miR-512-3p to study the possible functional role of miR-512-3p in MMD EVs were explored in MMD ECFCs. The potential targets of DEmiRNAs were analysed with differentially expressed mRNAs (DEmRNAs) using our previous ECFC mRNA array data (9) and then interrogated mRNA array data and target gene lists of miR-512-3p in TargetScan database (Fig. 3). Then, we focused on the target genes with binding sites to upregulated miR-512-3p and found a total of 14 downregulated genes showing negative correlation (Table 3). Among these predicted target genes, top 10 genes were verified through RT-qPCR. Rho Guanine Nucleotide Exchange Factor 3 (ARHGEF3), Glucoside Xylosyltransferase 1 (GXYLT1), Speckle Type BTB/POZ Protein (SPOP), Survival Motor Neuron Domain Containing 1 (SMNDC1) were significantly downregulated in MMD ECFCs which is consistent with the analysis data (Fig. 4). Unlike the analysis results, Thymocyte Selection Associated High Mobility Group Box (TOX) was upregulated in MMD ECFCs, and the rest of the genes were not significantly different with normal ECFCs. The most significantly downregulated gene was ARHGEF3.

Figure 3. The heatmap of the differential gene expression profiles in MMD and normal ECFCs

($\log_2$ fold change, $P < 0.05$).

Table 3. Targeted genes of miR-512-3p in MMD ECFCs.

| Target symbol	logFC	p-value	Key to Abbreviations and Symbols	Mechanism
ARHGEF3	-0.94857	6.44E-05	Rho Guanine Nucleotide Exchange Factor 3	GTPases regulation
TOX	-0.9426	5.64E-07	Thymocyte selection-associated high mobility group box	DNA binding, regulating T-cell development
PCDH10	-0.87165	8.89E-08	Protocadherin-10	Cell adhesion
PFKP	-0.54767	0.027887	Phosphofructokinase	Catalyzation of the phosphorylation of D-fructose 6-phosphate to fructose 1,6-bisphosphate by ATP
GXYLT1	-0.38038	0.00239	Glucoside Xylosyltransferase 1	UDP-xylosyltransferase activity
MBNL1	-0.35169	0.005029	Muscleblind Like Splicing Regulator 1	Pre-mRNA alternative splicing regulation
ARL5B	-0.28548	0.004888	ADP Ribosylation Factor Like GTPase 5B	GTPases regulation
SPOP	-0.25718	0.049932	Speckle-type BTB/POZ Protein	Ubiquitin protein ligase binding
SMNDC1	-0.24844	0.006545	Survival Motor Neuron Domain Containing 1	Spliceosome assembly
PTBP2	-0.23215	0.030718	Polypyrimidine Tract Binding Protein 2	Negative regulation of exons splicing.
SFMBT1	-0.17826	0.000555	Scm Like With Four Mbt Domains 1	Histone-binding protein
CUL1	-0.14358	0.028045	Cullin 1	Cell cycle
RSBN1L	-0.12393	0.0146	Round Spermatid Basic Protein 1 Like	Demethylation of methylated lysine residues
MBNL2	-0.11524	0.035313	Muscleblind Like Splicing Regulator 2	Pre-mRNA alternative splicing regulation
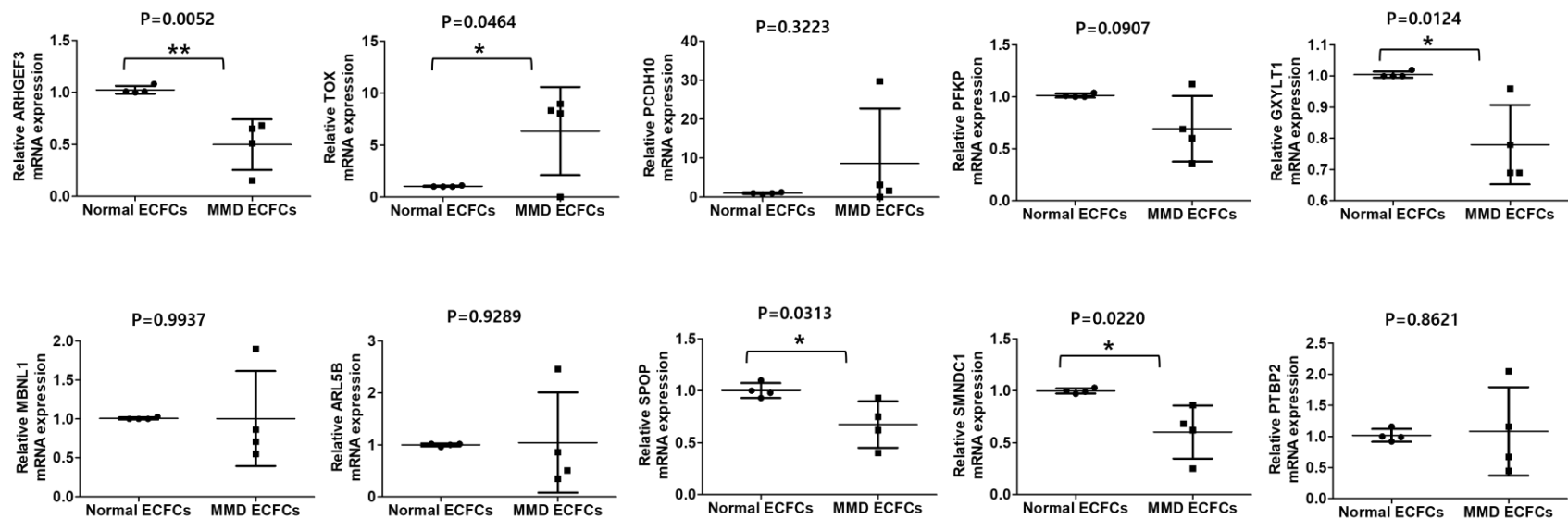
Figure 4. Verification of the mRNA expression targeted by miR-512-3p in MMD ECFCs.

According to the integrated analysis, 14 genes are expected to be targeted for upregulated miR-512-3p. Among them, 10 genes ranked verified expression patterns with RT-qPCR, and it is observed that the expression of ARHGEF3, GXYLT1, SPOP, and SMNDC1 is significantly reduced in MMD ECFCs compared to normal ECFCs (*: $p < 0.05$, **: $p < 0.01$).

No effect on MMD ECFCs viability by inhibition of miR-512-3p in MMD ECFCs

We investigated the effect of miR-512-3p in MMD ECFCs by miR-512-3p inhibition. We observed that transfection of miR-512-3p inhibitor into MMD ECFCs successfully reduced miR-512-3p by more than 50% in both MMD ECFCs12 and MMD ECFCs13 (Fig. 5A). The inhibition of miR-512-3p did not significantly affect cell viability in both MMD ECFCs12 and MMD ECFCs13 (Fig. 5B). We also confirmed that counts of miR-512-3p particles in EVs of MMD ECFCs were significantly decreased by miR-512-3p inhibitor through ExoView analysis (Fig. 5C).
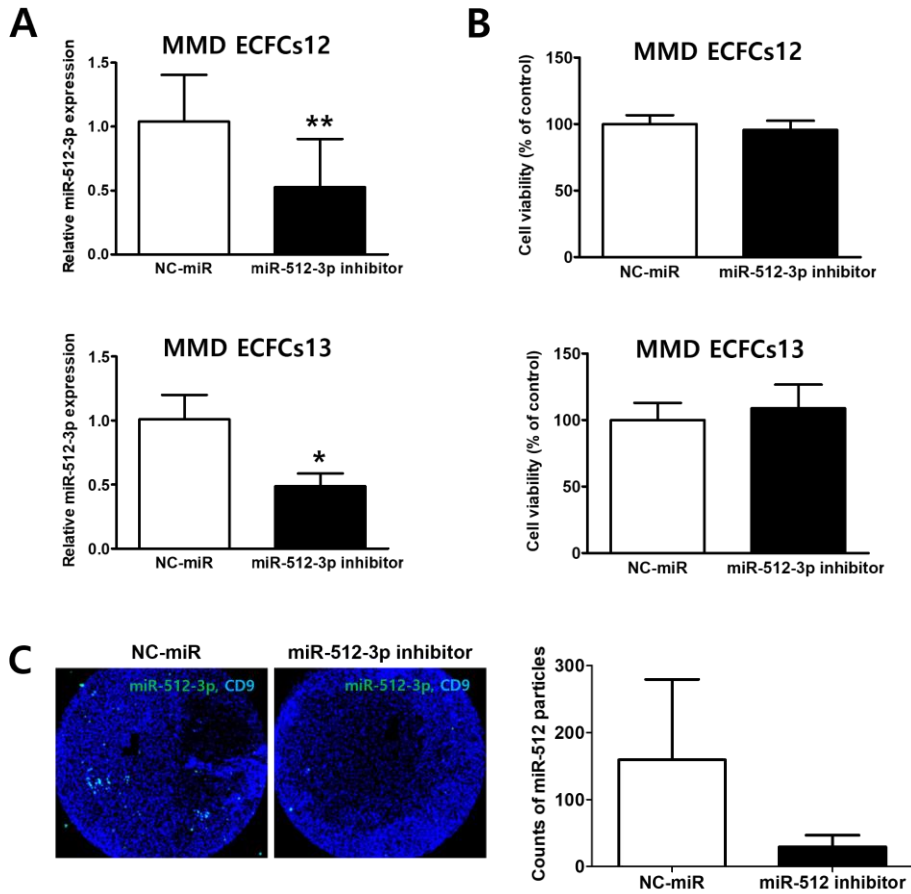
Figure 5. Inhibition of miR-512-3p in MMD ECFCs.

(A) After transfection with miR-512-3p inhibitor, miR-512-3p levels were significantly decreased in all MMD ECFCs. (B) There was no difference in cell viability by miR-512-3p inhibition in all MMD ECFCs. (C) ExoView analysis shows that miR-512-3p particles in EVs of MMD ECFCs are significantly decreased by miR-512-3p inhibitor (*: $p < 0.05$, **: $p < 0.01$).

Improvement of tubule formation by upregulation of ARHGEF3 by miR-512-3p inhibition in MMD ECFCs

We confirmed that the target gene ARHGEF3 was regulated by miR-512-3p inhibition. The inhibition of miR-512-3p increased ARHGEF3 mRNA level in MMD ECFCs by 3 times in MMD ECFCs12 and 1.5 times in MMD ECFCs13 (Figure 6A). We examined whether inhibition of miR-512-3p in MMD ECFCs regulates other target genes (GXYLT1, SPOP, and SMNDC1) of miR-512-3p (Fig. 6B). The expression of those genes was increased in MMD ECFCs12 by miR-512-3p inhibition, but there was no significant difference in MMD ECFCs13. We investigated the GTPase activity, which has been known to be regulated by ARHGEF3. As expected, we found that GTPase activity was improved (Figure 6C, NC-miR vs miR-512-3p inhibitor: 1.34 ± 0.02 vs 4.77 ± 0.02 mU/mg in ECFCs12, 1.35 ± 0.02 vs 1.84 ± 0.11 mU/mg in ECFCs13). Importantly, inhibition of miR-512-3p in MMD ECFCs were effectively increased the tubule formation ability by 1.5 times in MMD ECFCs12 and 3 times in MMD ECFCs13 (Fig. 6D). These results suggest that increase GTPase activity through upregulation of ARHGEF3 may promotes angiogenesis in MMD ECFCs.
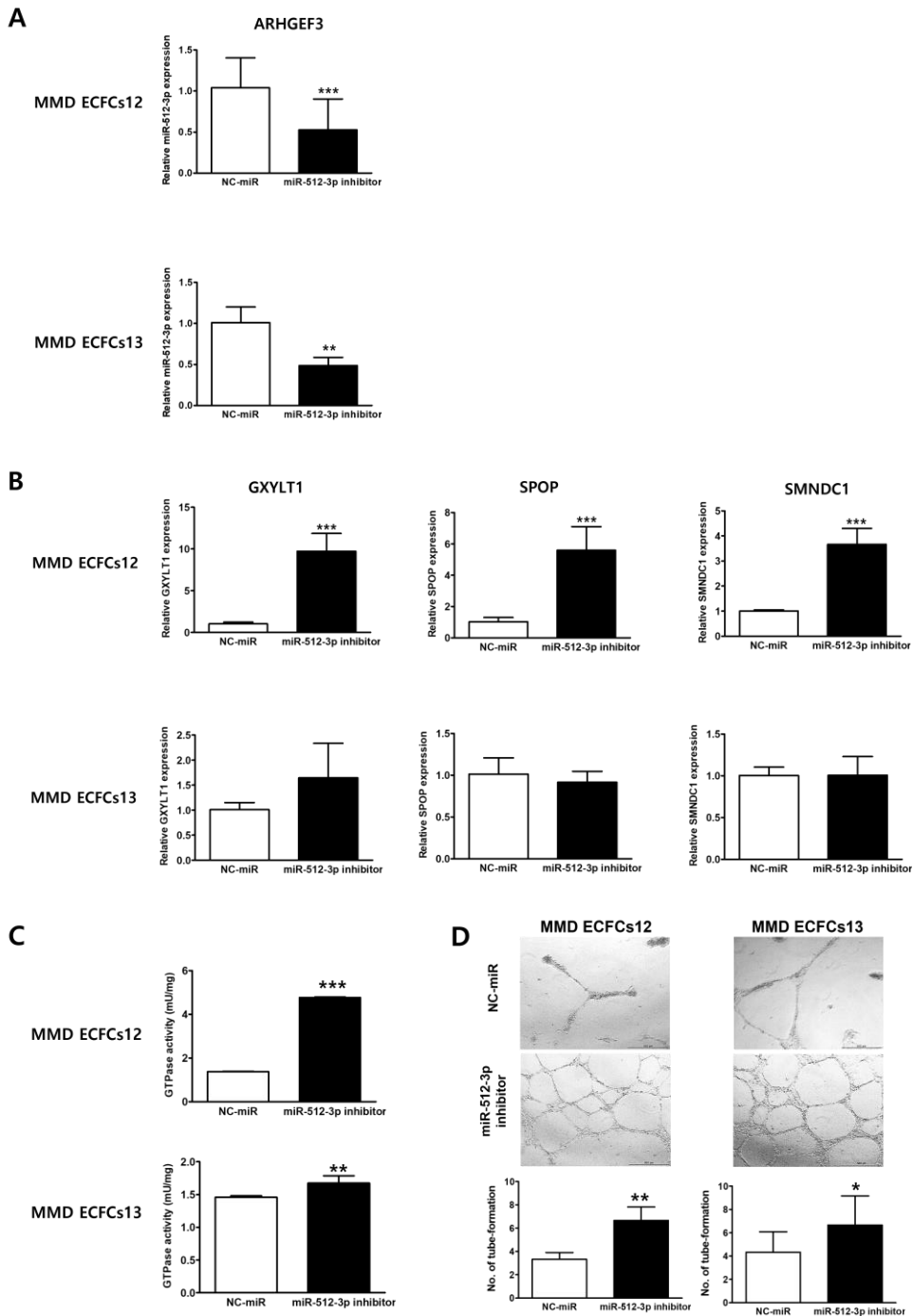
Figure 6. Transcripts levels of targeted genes, guanosine triphosphatase (GTPase) activity, and tubular formation ability after transfection with miR-512-3p inhibitor. (A) Expression levels of ARHGEF3 are significantly increased in all MMD ECFCs. (B) Expression levels of GXYLT1, SPOP, and SMNDC1 are significantly

25

increased in MMD ECFCs12. On the other hand, there is no significant difference in MMD ECFCs13. (C) GTPase activity are significantly increased in all MMD ECFCs. (D) Inhibition of miR-512-3p improves tubule formation ability in MMD ECFCs (*: $p < 0.05$, **: $p < 0.01$, ***: $p < 0.001$).

Discussion

In the present study, we identified 6 miRNAs expressed differentially in plasma-derived EVs from MMD patients compared to normal group. Among them, miR-512-3p was the only upregulated miRNA. At first, target gene ontology analysis was performed by integrating miR-512-3p and 5 miRNAs with low expression, but no meaningful results were obtained. Therefore, we focused on the highly expressed miR-512-3p and decided to search for genes downregulated by this miRNA. ROC analysis showed that miR-512-3p expression level in plasma-derived EV differentiated MMD and normal control with relatively good performance. ExoView analysis is relatively simple and quick method to verify EVs. To confirm whether the biomarker selected from plasma is also valid for CSF, we employed ExoView system to image and quantify miR-512-3p particles in CSF-derived EVs of MMD and control group. However, the number of captured miR-512-3p particles were significantly different between the two groups. For functional validation, ECFCs were cultured in the peripheral blood. MiR-512-3p showed higher expression in MMD ECFCs compared to normal ECFCs. Among target genes of miR-512-3p, ARHGEF3, GXYLT1, SPOP, and SMNDC1 were significantly downregulated in MMD ECFCs compared to normal ECFCs. When MMD ECFCs were treated with miR-512-3p inhibitors, ARHGEF3 was the only gene whose expression level was consistently increased in all MMD ECFCs used in the experiment. The treatment of miR-512-3p inhibitor boosted GTPase activity associated with ARHGEF3 and improved tubule formation in MMD ECFCs. Therefore, it can be inferred that miR-512-3p in plasma-derived EV cause angiogenic dysfunction by regulating ARHGEF3 in MMD ECFCs.

Previous studies revealed differentially expressed miRNAs and their target genes in blood or CSF of MMD patients. In 2014, Dai *et al*., reported the first study of a serum miRNA signature of MMD patients including upregulated miR-106b, miR-130a, miR-126 and downregulated miR-125-3p. Mammalian target of rapamycin

(mTOR) signaling was the most enriched pathway with functional target genes (12). Zhao et al. verified the expression and significance of let-7 family based on the existing literature, and among them, let-7c was confirmed to have the highest differential expression in serum of MMD compared to control group (13). A Taiwan group characterized the impact of the RNF213 mutations on plasma protein and RNA profiles. They analysed cell-free miRNAs in whole plasma, EV-encapsulated miRNAs, and EV-depleted miRNAs. Vascular endothelial growth factor (VEGF) signaling was the enriched pathway in mRNA-miRNA interaction (3). Uchino *et al*., performed MMD-discordant monozygotic twin-based study, miR-6722-3p, miR-328-3p were differentially upregulated in the plasma of MMD. Target genes downregulated in endothelial cells differentiated from induced pluripotent stem cell lines derived from MMD cohort were involved in Signal transducer and activator of transcription 3 (STAT3), Insulin like growth factor 1 (IGF-1), and Phosphatase and tensin homolog (PTEN) signaling (14). Wang *et al*., investigated CSF exosomal miRNA signature in MMD patients. The combination of miR-3679-5p, miR-165, miR-6750-5p and miR-574-5p showed a good performance (AUC=0.945) as a biomarker. The predicted target genes for the miRNAs were cell adhesion molecules, nectin 1 and contactin 2 (15). There was the study of CSF miRNA signature from MMD patients for predicting angiogenesis after indirect bypass surgery. miR-92a-3p, miR-486-3p, miR-25-3p, and miR-155-5p were significantly increase in the angiogenesis group compared to non-angiogenesis group (16). Various miRNA signatures were suggested through previous MMD research. Majority of molecular pathways affected by these miRNAs were related to angiogenesis. However, it was difficult to select a strong universal biomarker because the nationality, age, and clinical setting of the cohort in each study was different. The fact that miRNAs were searched for in EV, a more protective and consistent source of miRNA, can be advantage of this study, in comparison to earlier research employing cell-free serum/plasma or whole CSF (6).

We tried to validate MMD-specific miRNA of plasma-derived EV in CSF. ICA and its branches affected by MMD are vessels in the central nervous system (CNS). CSF is in closest contact with the CNS (15). Both blood and CSF may reflect the characteristics of the disease. Finding the intersection of blood and CSF biomarkers can be more convincing. We observed similar trend of miR-512-3p expression in CSF-derived EVs as in plasma-derived EVs through ExoView analysis, but the difference between normal and MMD was not statistically significant. Because we did not analyse full expression profiles of miRNA in CSF EVs, it was not confirmed whether miR-512-3p is included among the most highly expressed miRNAs in MMD CSF EVs compared to control group.

We used ECFCs as *in vitro* model for functional validation of miR-512-3p and its targets. Several *in vitro* experimental assays were designed to screen pro-/anti-angiogenic drugs. These assays measure the abilities of endothelial cells (ECs) regarding proliferation, migration, invasion, and the formation of tubular structures. Proliferation capacity of mature ECs decreases over time. Endothelial progenitor cells (EPCs) circulating peripheral blood have robust proliferation capacity and can be a source of tube formation assays. ECFCs are late EPCs. Circulating ECFCs are recruited to sites for vascular re on, and they are incorporated into the vascular endothelial lining and differentiated in situ into ECs (17). ECFCs play a critical role in the pathogenesis of MMD. The cell number and functioning of ECFCs were decreased or impaired in pediatric MMD patients (18).

ARHGEF3 belongs to the family of Rho-guanine nucleotide exchange factor which accelerates Rho-GTPase activity by conversion of GTP to Guanosine diphosphate (GDP). ARHGEF3 activates selectively two members of the Rho-GTPase family, RhoA and RhoB (19). ARHGEF3 is widely expressed in blood cells, skeletal muscle, and brain (20). ARHGEF3 is also an endogeneous mTOR complex 2 inhibitor (21). Mitogen-activated protein kinase (MAPK), phosphoinositide 3-kinase (PI3K), and mTOR pathway are downstream effectors in VEGF signaling.

29

Rho-proteins and their effectors function as key mediators of VEGF-mediated angiogenesis (13). The serine/threonine Rho-associated kinases (ROCKs) are RhoA effectors. RhoA/ROCK signaling increases vascular permeability, matrix-metalloproteases (MMPs)-mediated degradation of extracellular matrix through MAPK signaling, endothelial migration, proliferation by promoting G1/S transition, and morphogenesis (22). RhoA/ROCK signaling is also a key regulator of vascular contraction (23). ARHGEF3 may be involved in angiogenesis, activating Rho A/ROCK signaling. Downregulation of ARHGEF3 by miR-512-3p can play a role in the aberrant angiogenesis of MMD.

Our study has some limitations. There is an ethical problem in recruiting normal children as control cohort and collecting body fluids through an invasive procedure like blood sampling. The age range of normal group was in their early to mid-20s, thus it did not match the age of the patient group. Control groups were different in plasma-derived EV (young adults) and CSF-derived EV (children with hydrocephalus). We did not obtain CSF from normal group in plasma experiment. Even in young adults, collecting CSF from normal people via lumbar puncture is also very invasive. We did not inspect total profiles of differential expression of EV miRNAs with microarray or sequencing in CSF. Further experiments with CSF are needed in the future. In addition, ECFC mRNA microarray used for target gene analysis was previously constructed (9) and not derived from ECFCs of the patients in this study.

Conclusion

In summary, we identified that miR-512-3p was significantly upregulated in plasma-derived EVs of MMD patients compared to control group. Plasma-derived EV miR-512-3p showed a good performance as a diagnostic biomarker of MMD. We observed downregulation of ARHGEF3 gene targeted by miR-512-3p. miR-512-3p inhibition restored ARHGEF3 expression, GTPase activity and tubule formation in MMD ECFCs.

References

1.   Bersano A, Guey S, Bedini G, Nava S, Hervé D, Vajkoczy P, et al. Research Progresses in Understanding the Pathophysiology of Moyamoya Disease. Cerebrovasc Dis. 2016;41(3-4):105-18.

2.   Dlamini N, Muthusami P, Amlie-Lefond C. Childhood Moyamoya: Looking Back to the Future. Pediatr Neurol. 2019;91:11-9.

3.   Lee MJ, Fallen S, Zhou Y, Baxter D, Scherler K, Kuo MF, et al. The Impact of Moyamoya Disease and RNF213 Mutations on the Spectrum of Plasma Protein and MicroRNA. J Clin Med. 2019;8(10).

4.   Mori MA, Ludwig RG, Garcia-Martin R, Brandão BB, Kahn CR. Extracellular miRNAs: From Biomarkers to Mediators of Physiology and Disease. Cell Metab. 2019;30(4):656-73.

5.   Valadi H, Ekström K, Bossios A, Sjöstrand M, Lee JJ, Lötvall JO. Exosome-mediated transfer of mRNAs and microRNAs is a novel mechanism of genetic exchange between cells. Nat Cell Biol. 2007;9(6):654-9.

6.   Cheng L, Sharples RA, Scicluna BJ, Hill AF. Exosomes provide a protective and enriched source of miRNA for biomarker profiling compared to intracellular and cell-free blood. Journal of Extracellular Vesicles. 2014;3(1):23743.

7.   Kim KM, Abdelmohsen K, Mustapic M, Kapogiannis D, Gorospe M. RNA in extracellular vesicles. Wiley Interdiscip Rev RNA. 2017;8(4).

8.   Jangra A, Choi SA, Koh EJ, Moon YJ, Wang KC, Phi JH, et al. Panobinostat, a histone deacetylase inhibitor, rescues the angiogenic potential of endothelial colony-forming cells in moyamoya disease. Childs Nerv Syst. 2019;35(5):823-31.

9.   Lee JY, Moon YJ, Lee HO, Park AK, Choi SA, Wang KC, et al. Deregulation of Retinaldehyde Dehydrogenase 2 Leads to Defective Angiogenic Function of Endothelial Colony-Forming Cells in Pediatric Moyamoya Disease. Arterioscler Thromb Vasc Biol. 2015;35(7):1670-7.

10.   Choi SA, Koh EJ, Kim RN, Byun JW, Phi JH, Yang J, et al. Extracellular vesicle-associated miR-135b and -135a regulate stemness in Group 4 medulloblastoma cells by targeting angiomotin-like 2. Cancer Cell Int. 2020;20(1):558.

11.   Kuravi SJ, Yates CM, Foster M, Harrison P, Hazeldine J, Hampson P, et al. Changes in the pattern of plasma extracellular vesicles after severe trauma. PLOS ONE. 2017;12(8):e0183640.

12.   Dai D, Lu Q, Huang Q, Yang P, Hong B, Xu Y, et al. Serum miRNA signature in Moyamoya disease. PLoS One. 2014;9(8):e102382.

13.   van Nieuw Amerongen GP, Koolwijk P, Versteilen A, van Hinsbergh VW. Involvement of RhoA/Rho kinase signaling in VEGF-induced endothelial cell migration and angiogenesis in vitro. Arterioscler Thromb Vasc Biol. 2003;23(2):211-7.

14.   Uchino H, Ito M, Kazumata K, Hama Y, Hamauchi S, Terasaka S, et al. Circulating miRNome profiling in Moyamoya disease-discordant monozygotic twins and endothelial microRNA expression analysis using iPS cell line. BMC Med Genomics. 2018;11(1):72.

15.   Wang G, Wen Y, Faleti OD, Zhao Q, Liu J, Zhang G, et al. A Panel of Exosome-Derived miRNAs of Cerebrospinal Fluid for the Diagnosis of Moyamoya Disease. Frontiers in Neuroscience. 2020;14.

16.   Wang G, Wen Y, Chen S, Zhang G, Li M, Zhang S, et al. Use of a panel of four microRNAs in CSF as a predicted biomarker for postoperative neoangiogenesis in moyamoya disease. CNS Neurosci Ther. 2021;27(8):908-18.

17.   Lee H, Kang K-T. Advanced tube formation assay using human endothelial colony forming cells for in vitro evaluation of angiogenesis. kjpp. 2018;22(6):705-12.

18.   Kim JH, Jung JH, Phi JH, Kang HS, Kim JE, Chae JH, et al. Decreased level and defective function of circulating endothelial progenitor cells in children with moyamoya disease. Journal of neuroscience research. 2010;88(3):510-8.

19.   Liu TH, Zheng F, Cai MY, Guo L, Lin HX, Chen JW, et al. The putative tumor activator ARHGEF3 promotes nasopharyngeal carcinoma cell pathogenesis by inhibiting cellular apoptosis. Oncotarget. 2016;7(18):25836-48.

20.   Liao L, Qian ZY, Li XY, Yang DS, Lei BJ, Li HJ, et al. Disrupting RhoA activity by blocking Arhgef3 expression mitigates microglia-induced neuroinflammation post spinal cord contusion. J Neuroimmunol. 2021;359:577688.

21.   Khaliq SA, Umair Z, Yoon M-S. Role of ARHGEF3 as a GEF and mTORC2 Regulator. Frontiers in Cell and Developmental Biology. 2022;9.

22.   Bryan BA, D'Amore PA. What tangled webs they weave: Rho-GTPase control of angiogenesis. Cell Mol Life Sci. 2007;64(16):2053-65.

23.   Nunes KP, Webb RC. New insights into RhoA/Rho-kinase signaling: a key regulator of vascular contraction. Small GTPases. 2021;12(5-6):458-69.

국문초록

배경: 모야모야병은 뇌혈관의 협착이 진행하는 질환으로 소아에서 뇌졸중의 주 원인으로 알려져 있다. 세포밖소포체에 탑재된 마이크로리보핵산이 세포간 전달에 있어 중요한 역할을 하고 질병의 발생과 진행에 영향을 미친다는 연구들이 보고되고 있다. 본 연구에서는 소아 모야모야병 환자의 혈장에서 유래된 세포밖소포체 탑재 마이크로리보핵산에 대해 분석하고, 이 질환의 병태생리에서 어떤 역할을 하는지 살펴보고자 한다.

방법: 소아 모야모야병 환자 및 젊은 건강한 성인을 대상으로 말초혈액을 채취하여 혈장을 분리하고, 혈장에서 세포밖소포체를 분리하였다. 정상군과 비교하여 환자군에서 차별 발현하는 세포밖소포체 내의 마이크로리보핵산을 확인하고, 환자 혈액에서 배양한 혈관내피전구세포의 메신저리보핵산 발현 결과와 매칭하여 해당 마이크로리보핵산이 표적하는 유전자를 확인하였다. 혈관내피전구세포에서 이 마이크로리보핵산의 억제제를 처리할 때 세포의 생존능, 표적 유전자의 발현 정도, 혈관형성능, GTPase 활성 정도의 변화를 확인하였다.

결과: 혈장 유래 세포밖소포체를 특성화분석 했을 때 정상군, 환자군 모두 세포밖소포체의 특성에 차이가 없음을 확인하였다. 마이크로핵산의 발현을 분석했을 때 정상군과 비교하여 환자군에서 miR-512-3p가 가장 높게 발현하였다. 이 마이크로핵산의 발현량으로 수신자 조작 특성 곡선을 그리고 곡선 아래 면적을 분석했을 때 0.823로 모야모야병의 진단 바이오마커로서의 활용 가능성

을 확인하였다. miR-512-3p의 표적 유전자 중 환자 혈관내피전구세포에서 가장 낮게 발현한 것은 ARHGEF3였다. 혈관내피전구세포에 miR-512-3p의 억제제를 처리하였을 때 세포의 생존능에는 영향을 주지 않았고, ARHGEF3의 발현이 증가했으며, 혈관 형성, GTPase 활성도 증가하였다.

결론: 소아 모야모야병 환자의 혈장 유래 세포밖소포체 탑재 miR-512-3p는 ARHGEF3를 억제하여 혈관내피전구세포의 혈관 형성능에 영향을 준다.